Modeling Contaminant Transport and Biodegradation in a Layered System

Brian D. Wood
Clint N. Dawson
Jim E. Szecsody
Gary P. Streile

March, 1993

TR93-12

MODELING CONTAMINANT TRANSPORT AND BIODEGRADATION IN A LAYERED SYSTEM

Brian D. Wood*
Clint N. Dawson**
Jim E. Szecsody*
Gary P. Streile*

February, 1993

Submitted to: *Water Resources Research*

Work supported by the
U.S. Department of Energy
under Contract DE-AC06-76RLO 1830

*Geosciences Department
Pacific Northwest Laboratory
Richland, Washington, 99352

**Department of Mathematical Sciences
Rice University
Houston, Texas, 77001

ABSTRACT

The transport and biodegradation of an organic compound (quinoline) were studied in a system of layered porous media to examine the processes that affect microbial growth near hydraulic layer interfaces. From a set of independent experiments, a mathematical model for the microbial kinetics was developed to describe the time rate of change of the concentrations of two organic compounds (quinoline and its first degradation product), one electron acceptor (oxygen), and microorganisms. This mathematical model was incorporated into a two-dimensional numerical model for flow and transport, so that simulations of the laboratory system could be conducted and results compared with the observed data. The model was formulated from the single-phase perspective (i.e., it did not include mass-transfer limitations between the aqueous and microbial phases). These comparisons suggest that, for some systems, a single-phase model can adequately describe the reactive processes that occur between aqueous components and microorganisms. Microbial lag was explicitly accounted for in the degradation kinetics. For the system described here, the inclusion of microbial lag was important for describing transient concentration pulses observed in the low-conductivity layer.

INTRODUCTION

The possibility of using microorganisms to remediate subsurface contaminants has been recognized for some time, and the existence and metabolic abilities of subsurface organisms have been documented in an

extensive and growing literature summarized by *Madsen* [1991]. Recent discoveries of metabolically diverse microorganisms in many different subsurface environments [e.g., *Balkwill et al.*, 1989; *Colwell*, 1989; *Fredrickson et al.*, 1991; *Severson et al.*, 1992] have helped to foster increased interest in bioremediation as a feasible technology. Many of these subsurface organisms have been shown to have unique abilities to degrade highly refractory organic compounds [*Madsen and Ghiorse*, 1992], and thus may be particularly useful for remediation.

An important part of developing the use of native subsurface microorganisms in remediation technologies will be to understand the processes that affect the growth of these organisms. Despite the developing interest in subsurface bioremediation, there is still a lack of fundamental information about how to properly represent microbiological reactions involving dissolved aqueous species in groundwater. Much of this lack stems from the fact that, although many conceptual models have been proposed for simulating microbial degradation of organic compounds in porous media [e.g., *Sykes et al., 1982; Bouwer and McCarty, 1984; Borden and Bedient, 1986; Moltz et al., 1986; Kindred and Celia, 1989*], few field or laboratory data have been collected to verify these models.

A number of mathematical models have been developed that couple unstructured microbial growth kinetics with the transport of bioactive components in groundwater systems. These models can be broadly grouped into two categories: 1) those that include mass-transfer limitations between the fluid phase and the microbes (hereafter referred to as "multiple-phase models"), and 2) those that assume that the mass-transfer limitation between the biomass and the aqueous phase can be neglected (hereafter referred to as "single-phase models"). Multiple-phase models include those of *Rittman et*

al. [1980], *Bouwer and McCarty* [1984], *Widdowson et al.* [1988], and *Kinzelbach et al.* [1991]. These models separate the biomass and aqueous phases and assume that there is a mass-transfer limitation between them, making these formulations mathematically similar to the mobile/immobile region models that have been used by groundwater and soils scientists for some time [e.g., *Coats and Smith,* 1964; *van Genuchten and Wierenga,* 1976; *De Smedt and Wierenga,* 1979; *Valocchi,* 1985]. Single-phase models have been used more widely in applications to bioremediation; examples of these models can be found in *Sykes et al.*[1982], *Bouwer and McCarty* [1984], *Borden and Bedient* [1986], *Kindred and Celia* [1989], *Baveye and Valocchi* [1989], and *Chiang et al.* [1989].

The research described here is part of a broader effort that focuses on the integrated effects of microbiology in simple heterogeneous (layered) flow systems. The purpose of the work described in this paper is to examine conceptual and mathematical descriptions of microbial growth and degradation kinetics in a porous media system. In particular, we are interested in determining whether a single-phase model for microbial kinetics that was developed independently of the system under investigation could be applied to give accurate predictions of the transport of reactive dissolved aqueous species.

Although no formal review of microbiology or microbial kinetics is given here, interested readers are referred to the brief introduction to these topics (as applied to modeling subsurface flow and transport) offered by *Kindred and Celia* [1989]; more extensive information is available in the texts of *Baily and Ollis* [1986], *Roels* [1983], and *Gaudy and Gaudy* [1988].

EXPERIMENTAL METHODS

Description of Experimental System

A 2-dimensional transport and biodegradation experiment was conducted in a saturated rectangular flow cell containing a layered porous medium (Figure 1). The flow cell was 1 m long by 0.2 m high by 0.1 m wide, and was constructed of stainless steel (304L) with Teflon seals to minimize interactions with solutes. Advection was along the horizontal (lengthwise, 1-m) dimension (x coordinate), and transverse directions were z (vertical, 0.20 m) and y (lateral, 0.1 m). The porous medium was composed of silica sand placed in two hydraulic layers with a ratio of conductivities (as packed in the flow cell) of approximately 1:13; the high-conductivity layer (high-K) was 3 cm thick and the low-conductivity layer (low-K) 17 cm thick. The hydraulic conductivities of the porous medium were chosen such that there would be rapid advective transport in the high-K layer, and a relatively large transverse dispersion flux in the low-K layer. The pore-water velocity was 124 cm d^{-1} in the high-K layer and 9.5 cm d^{-1} in the low-K layer.

During packing, the flow cell medium was inoculated with an initial microbe concentration of approximately 5×10^6 colony-forming units (CFU) per gram of dry sand in the low-K layer; no microbes were packed in the high-K layer initially. The microorganism used for these experiments was a bacterium (*Pseudomonas cepacia*, strain 866A [*R. Reeves*, reported by *Truex et al.*, 1992]) isolated from the subsurface at Savannah River, GA, at a depth of 203 m. This organism (herafter referred to as 866A), has the capability to degrade quinoline [*Brockman et al.*, 1989], a nitrogen-heterocyclic compound that is associated with fossil-fuel processing [*Pereira et al.*, 1983; *Stuermer et al.*, 1987], as its sole source of energy, carbon, and nitrogen. The details of the quinoline degradation kinetics of 866A relative to modeling are described in

more detail below.

Quinoline and salt tracers were introduced into the flow cell as a planar solute front from the injection end of the flow cell (Figure 1). Injection of these aqueous components continued at a constant rate for the duration of the experiment (approximately 515 hours). Concentrations of quinoline, its first degradation product 2-hydroxyquinoline (hereafter referred to as 2OHQ), oxygen, and tracers were monitored over time at various locations in the flow cell through sampling ports installed in the flow cell walls. Ports were located in a grid with a vertical spacing of 3-6 cm and horizontal spacing of 5-10 cm. The ports were constructed to accept a flat-bottomed tubing fitting, into which was inserted a sterile 20-gauge needle and needle valve; sampling needles were placed so that the needle tip was located along the longitudinal center of the flow cell. During the course of the experiment, samples of approximately 0.5 ml were withdrawn aseptically using gas-tight borosilicate glass syringes for analysis by high-pressure liquid chromatography (HPLC); accuracy of the HPLC analysis was $\pm$ 0.5 mg L^{-1}.

Collection of Model Parameters

Microbial kinetic parameters were determined in batch and column experiments conducted in support of the larger-scale experiments. Batch experiments were conducted to determine the values for the maximum specific growth rate (μ_m), the yield coefficient (Y), the ratio of oxygen consumed to substrate consumed (f), and the parameters that describe microbial lag (τ_L and τ_E). (The mathematical model of the microbial kinetics and its associated parameters are described in more detail below.) Because growth of bacteria in porous media might be expected to have different characteristics from growth of planktonic bacteria in batch systems,

experiments were also performed in columns packed with glass beads to examine the effects of porous media on the parameters μ_m, Y, τ_L, and τ_E.

In batch systems, growth parameters were determined using 5-, 20- and 100-ppm initial 2OHQ concentrations. Because the initial degradation step (from quinoline to 2OHQ) does not result in growth of the organism, the kinetic parameters were determined using 2OHQ as the initial substrate; additional data for the kinetics of the first step of the degradation sequence (quinoline transformation to 2OHQ) were based on data from *McBride et al.* [1992] and *Malmstead* [1992]. Washed cells (~10^5 CFU ml^{-1} in 25 ml of sterile mineral salts) were dispensed to three sterile, screw-top Erlenmeyer flasks. Cells in one flask were autoclaved and the volume was readjusted to 25 ml with sterile mineral salts to provide a control. Then 2OHQ at twice the desired concentration was added to each flask to give a final volume of 50 ml at the desired concentration. Periodically 0.6-ml samples were withdrawn, and the number of culturable bacteria was determined in duplicate on 10% tryptic soy agar spread plates. The remaining sample was centrifuged (10,000 x g, 6 min) and the supernatant (2 ml) analyzed for 2OHQ concentration by HPLC.

The stoichiometric amount of oxygen used for the degradation of 2OHQ was determined in similar batch experiments, using the procedures above. Washed cells (~10^5 CFU ml^{-1} in 25 ml of sterile mineral salts) were added to a respiration flask equipped with a calibrated oxygen probe; 2OHQ was added to make a final concentration of 1 ppm. The changes in dissolved oxygen concentration were measured after the metabolism of the substrate was complete and were used to calculate the mass of oxygen used per unit mass of substrate

In the column systems, growth parameters were determined at 20- and

100-ppm 2OHQ influent concentrations using five separate columns. The experimental arrangement for these columns was similar to that used by *McBride et al.* [1992]. An initial cell density of ~10^5 CFU per gram of glass beads was used, and inoculated beads were aseptically packed in glass chromatography columns (2.5-cm inside diameter) to a length of 1 cm. Beads were constrained in the column by plunger assemblies fitted with filters (30- to 60-μm pore size). All column components and tubing were autoclaved or soaked in disinfectant (5% Roccal II) overnight and thoroughly rinsed with sterile mineral salts before use. Sterile 2OHQ feed solutions were contained in autoclaved feed bottles.

A constant flow rate (supplied by HPLC-type piston pumps) resulting in a 10-minute fluid residence time for each column. Influent samples were collected during experiments and analyzed by HPLC to ensure a constant 2OHQ influent concentration. The concentration of 2OHQ in the effluent of one column was continuously measured by ultraviolet (UV) absorbance; in all five columns, periodic effluent samples from each column were collected and 2OHQ concentrations analyzed by HPLC. Each column was removed in sequence from the system for measurement of the microbial concentration in the porous medium; in this way a sequence of microbial concentrations over time was obtained. The glass beads and inlet and outlet plunger filters from the column were collected, and microbial biomass concentrations were measured by protein analysis [cf. *Truex et al.*, 1992]

Before the biodegradation experiment was conducted in the 2-layer silica sand system, transverse dispersion was measured in an experiment that consisted of a continuous point-source injection of a 40 mmol L^{-1} $CaCl_2$ solution (at 1.01 cm^3 min^{-1}) into the flow cell. The tracer was injected into the low-*K* layer (fine sand) at a point 60 cm from the inlet end, and fluid

samples were taken periodically at three locations directly downgradient of the injection point (at x = 70, 80, and 90 cm) until a steady-state concentration was reached. The transverse dispersivity was calculated as described by *Robbins* [1989]. The 3-cm-thick, high-K layer was too thin for conducting a similar point injection experiment in this 2-layer system to obtain intralayer dispersion parameters for that medium. Therefore two similar point-injection experiments were conducted in another flow cell packed with only the coarse silica sand.

Plane-source injection experiments were also conducted in the flow cell specifically to measure longitudinal dispersion within each layer. Tracer concentration was measured over time at three locations in the low-K layer (far from the influence of the interface). As with the transverse dispersivity measurement, breakthrough curves for the determination of the longitudinal dispersivity were obtained for the high-K medium in a separate experiment, in a flow cell packed with only the coarse silica sand. Longitudinal dispersivities were determined by conducting a nonlinear least-squares fit of the breakthrough curve data, as described by *Parker and van Genuchten* [1984].

Model Formulation

Microbial kinetics in porous media

In the environment, the growth kinetics of microorganisms may be a function of a large set of environmental variables (e.g., nutrient concentrations, pH, temperature, competition with other organisms) and may also be regulated by the history of environmental conditions

experienced by the organism. In application, however, the mathematical description of microbial kinetics in the environment must use a substantially reduced set of variables, because developing an exact mechanistic description of microbial processes is a formidable problem. In the process of making the mathematical description of microbial kinetics tractable, some empiricism is introduced [*Roels*, 1983]; however, observations in many natural and artificial systems have shown that this semi-empirical approach is often adequate for the description of microbial growth and changes in associated aqueous-phase species, so these models are widely applied.

Models used to describe microbial kinetics can be categorized as being either structured or unstructured. Structured models [e.g., *Williams*, 1967; *Ramkrishna et al.*, 1967; *Pamment et al.*, 1978] are generally more mechanistic and represent physiological changes in the cell by expressing the kinetics in terms of variables both internal (e.g., concentration of enzymes, DNA, RNA, ATP) and external to the cell (i.e., environmental variables). Unstructured models describe microbial growth as a function of environmental variables and cell concentration only; internal changes in cellular biochemistry are not accounted for in a mechanistic sense. Application of structured models tends to be somewhat complicated; therefore, models applied to problems in the environment have been largely of the unstructured type. The potential use of structured models in porous media has been discussed briefly by *Baveye and Valocchi* [1989]. As our knowledge of microbial growth in porous media increases, these models may provide a better means of describing microbial processes in subsurface environments.

For applications to groundwater systems, variations of the unstructured

kinetic model proposed by *Monod* [1949] have been used. A modification of the Monod model [*MeGee et al.*, 1970] describes the specific growth rate as a function of the concentration of one or more limiting nutrients:

$$\mu = \mu_m \left[\frac{C_1}{C_1 + K_1}\right]\left[\frac{C_2}{C_2 + K_2}\right]\cdots\left[\frac{C_i}{C_i + K_i}\right] \tag{1}$$

where C_i [M L^{-3}] represents the concentrations of one or more limiting nutrients (which may be substrates or electron acceptors), μ_m [T^{-1}] is the maximum specific growth rate of the biomass, and K_i [M L^{-3}] is the substrate half-saturation constant. For the purposes of this work, the term "nutrient" is defined as any element or compound required for growth of an organism [after *Lee*, 1992]. During microbial growth, one or more nutrients will limit growth, and other nutrients will be present in excess; the term "limiting nutrients," then, is applied to the subset of nutrients that limit the rate of growth. Although the Monod model has been successfully applied to a wide variety of problems, it is empirically based, and in some cases other models, such as those proposed by *Contois* [1959], *Moser* [1958], and *Dabes et al.* [1973], may yield better results [*Edwards*, 1970; *Dabes et al.* 1973; *Roels* 1983].

In general, the mathematical model used to describe the kinetics of a particular system should be based on phenomenological considerations of that system. The model should incorporate each of the phenomena that are known or expected to have a significant effect on microbial growth. In addition to the effect of nutrient limitation, which is accounted for by such approaches as the Monod model, other effects which may profoundly influence microbial kinetics include enzyme inhibition, production of metabolic toxins, the occurrence of a lag before substrate degradation can begin, and competition between microbial species. Although there are

mathematical methods to describe each of these phenomena separately, no single kinetic model can be generalized to describe microbial growth for all systems; it is necessary, therefore, to develop kinetics models specific to the systems of interest. The microbial kinetics for the flow cell system described herein have been developed with this type of approach and are described in more detail below.

Formulation of Mathematical Model

The development of a multiple-phase kinetic model results in a set of coupled equations to describe mass transport in mobile aqueous and immobile biomass phases and the growth of the biomass phase [e.g., *Baveye and Valocchi,* 1989]. Although the conceptualizations of the physical distribution of biomass may be somewhat different among these models, they all require a mass-transfer coefficient that allows representation of the pore-scale mass-transfer process at the macroscopic scale at which the associated mass-balance equations are valid. Because these mass-transfer coefficients are dependent on geometrical configurations of the biomass and must reflect the effects of averaging the pore-scale mass-transfer process up to the macroscopic scale, their physical interpretation may be difficult.

In contrast, the single-phase formulation assumes that the mass-transfer limitation between the biomass and the aqueous phase can be neglected. This leads to mass-balance equations that are written for a single aqueous phase and do not require the estimation of additional parameters to describe interphase transfer. This formulation can be applied only when it can be shown that mass-transfer limitations can be neglected.

It can be shown that, for large values of the mass-transfer coefficient, the multiple-phase models reduce to a single-phase model; this result is

described in the Appendix. The purpose of the models developed here is to simulate the results of experiments that were conducted at low microbial concentrations, where mass-transfer limitations between the aqueous phase and biomass were negligible. The model formulated below is written from a single-phase perspective for simplicity.

A macroscopic mass-balance equation for an aqueous-phase component i subject to advection, dispersion, and reactions can be written as

$$\frac{\partial(\theta_w C_i)}{\partial t} = \nabla \bullet (\theta_w \mathbf{D}_i \nabla C_i - \theta_w \mathbf{V} C_i) + \Gamma_i \qquad (2)$$

where for each component i, θ_w is the volumetric water content, C_i is the aqueous concentration, $\mathbf{D}_i$ is the dispersion tensor, $\mathbf{V}$ is the velocity vector, and Γ_i is a net source/sink term for reactions.

Equations in the form of (2) can be written for each aqueous-phase species of interest. For systems that include biological reactions, an equation in the form of (2) must be written for each aqueous species which has been included in the mathematical description of the microbial kinetics. For the experimental system described above, in which there are two biologically reactive organic components (quinoline and 2OHQ; below, S_1 and S_2, respectively), one biologically reactive inorganic component (oxygen; below, O), and microorganisms (below, X), equation (2) can be written for these three components as

$$\frac{\partial(\theta_w S_1)}{\partial t} = \nabla \bullet (\theta_w \mathbf{D}_{S1} \nabla S_1 - \theta_w \mathbf{V} S_1) + \Gamma_{S1} \qquad (3a)$$

$$\frac{\partial(\theta_w S_2)}{\partial t} = \nabla \bullet (\theta_w \mathbf{D}_{S2} \nabla S_2 - \theta_w \mathbf{V} S_2) + \Gamma_{S2} \qquad (3b)$$

$$\frac{\partial(\theta_w O)}{\partial t} = \nabla \bullet (\theta_w \mathbf{D_O} \nabla O - \theta_w \mathbf{V} O) + \Gamma_O \tag{3c}$$

$$\frac{\partial(\theta_w X)}{\partial t} = \Gamma_X \tag{3d}$$

At the velocities used for these experiments, the microorganism used in this research remains strongly attached to the solid phase [*Truex et al.*, 1992]; therefore, there are no advection or dispersion terms for the microbial phase in equation (3d).

For the system described here, flow is parallel to the horizontal (x) direction, and the principal values of dispersion occur on the diagonal elements of the dispersion tensor. These values are represented as $D_{xx} = \alpha_L V_x + D_i^*$ and $D_{zz} = \alpha_T V_x + D_i^*$ in the x and z directions respectively, where α_L and α_T are the lateral and transverse dispersivities [L], and D_i^* is the molecular diffusion coefficient for component i in the porous medium [L^2 T^{-1}] [*Bear*, 1972].

The system of equations given by (3), in addition to the proper initial and boundary conditions, can be solved provided the source/sink terms (in the form of microbial kinetic expressions) are functions of S_1, S_2, and O only. The formulation of kinetic expressions for the reaction terms in equations (3) are described below.

Quinoline Degradation Reaction

Based on research of *Brockman et al.* [1989] and *Malmstead* [1992], the aerobic degradation pathway of quinoline can be represented by the reaction sequence shown in Figure 2 [adapted from *Malmstead*, 1992]. This degradation sequence is for the complete catabolic degradation of quinoline; carbon that is used in anabolic pathways or incorporated into cellular

macromolecules and carbon that is left in refractory end products are not accounted for in this reaction. Although the pathway for quinoline degradation by the organisms used in this research has multiple intermediates, the concentrations of only quinoline and 2OHQ were measured during the experiment. Batch experiments showed that increases in microbial cell concentration correlated well with decreases in the concentration of 2OHQ over the entire range of growth, and no growth was observed after 2OHQ was exhausted. These results suggest that the degradation steps that occur after the degradation of 2OHQ occur quickly and can be considered instantaneous. The degradation of quinoline (accounting for catabolic processes, fixation of carbon, and end-product formation) can then be represented by the following set reactions:

$$C_9H_7N + H_2O \longrightarrow C_9H_6NOH + 2H^+ + 2e^- \qquad (4a)$$

$$C_9H_6NOH + aO_2 + bH_2O \longrightarrow$$

$$cCO_2 + dH^+ + de^- + eNH_3 + fC_5H_7O_2N + \text{End Products} \qquad (4b)$$

where C_9H_7N is the molecular formula for quinoline, C_9H_6NOH is the molecular formula of 2OHQ, $C_5H_7NO_2$ is an empirical representation of the molecular formula for microbial mass [*Gaudy and Gaudy*, 1988], and lower-case letters represent stoichiometric coefficients. Although no oxygen is shown to be directly consumed in reaction (4a), some researchers have suggested that the hydrogen ions produced by this step are combined with molecular oxygen to produce water [*Malmstead*, 1992], resulting in an indirect use of oxygen at this step.

Initial analysis of both batch and column experiments indicated that for quinoline and 2OHQ, there was a lag between the time that microbes

encountered the substrates and the time the substrates began to be degraded. Such a delayed response is often observed for substrates that are somewhat refractory, and this lag represents a period during which the microbial population must induce the enzymatic pathway necessary for degrading the introduced compounds. In cases where microbial lag is appreciable, the microbial kinetics are a function not only of the concentrations of limiting nutrients, but also of the total time in contact with a subset of these nutrients [e.g., *Powell*, 1967]. Therefore, in addition to incorporating substrate and electron acceptor limitations, the kinetic models developed here include the effects of microbial lag. None of the aqueous-phase components reacted with the surface of the silica sand, so for this system the effects of sorption are not included in the source/sink terms.

The equations proposed to describe the kinetics of quinoline degradation for our flow cell system are as follow:

$$\Gamma_{S1} = -kXS_1\left(\frac{O}{O+K_{O1}}\right)\lambda \tag{5a}$$

$$\Gamma_{S2} = -\frac{\mu}{Y}X\left(\frac{S_2}{S_2+K_{S2}}\right)\left(\frac{O}{O+K_{O2}}\right) - r\Gamma_{S1} \tag{5b}$$

$$\Gamma_O = -kf_1S_1X\left(\frac{O}{O+K_{O1}}\right)\lambda - \frac{\mu f_2 X}{Y}\left(\frac{S_2}{S_2+K_{S2}}\right)\left(\frac{O}{O+K_{O2}}\right) - \gamma X \tag{5c}$$

These expressions are the source/sink terms for equations (3) above. In addition, an expression for the growth rate of microorganisms is required:

$$\Gamma_X = \mu X\left(\frac{S_2}{S_2+K_{S2}}\right)\left(\frac{O}{O+K_{O2}}\right) - bX \tag{5d}$$

where

k first-order reaction rate coefficient for quinoline reaction (4a) [T-1]

X mass of microorganisms attached to solids per unit volume porous medium [M L3]

$S_{1,2}$	fluid phase concentrations of quinoline and 2OHQ, respectively [M L3]
O	fluid phase concentration of oxygen (electron acceptor) as molecular O_2 [M L3]
$K_{O1,O2}$	half-saturation constants for oxygen [M L3]
λ	function accounting for metabolic lag
μ	specific growth rate [T-1]
Y	yield coefficient (mass of organisms created per unit substrate consumed)
K_{S2}	half-saturation constant for 2OHQ [M L3] for reaction (4a)
r	ratio of mass of 2OHQ produced per unit mass of quinoline degraded
f_1	ratio of mass of oxygen consumed per unit mass quinoline consumed
f_2	ratio of mass of oxygen consumed per unit mass 2OHQ consumed
γ	endogenous respiration oxygen utilization coefficient
b	microbial decay / endogenous respiration coefficient [T-1]

The metabolic lag function λ is based on a description of lag for batch systems by *Kono* [1968], and is described in detail by *Wood and Dawson* [1992]. The function is given by

$$\lambda = \begin{cases} 0, & t < \tau_L \\ \dfrac{\tau - \tau_L}{\tau_E - \tau_L}, & \tau_L \le t \le \tau_E \\ 1, & t > \tau_E \end{cases} \qquad (6)$$

where τ [T] is the time that microorganisms in a given volume have been in contact with the inducing substrate, τ_L [T] is the lag time, and τ_E [T] is the length of time required to reach exponential growth.

Equation (5a) represents the degradation rate of quinoline; equation (5b) represents the net rate of change of 2OHQ, which is the sum of the rate of production of 2OHQ obtained from equation (5a), and the rate of degradation

of 2OHQ to CO_2 and water. Equation (5c) expresses the rate of oxygen uptake from the degradation of 2OHQ and indirectly from hydrogen ions produced in the quinoline to 2OHQ step. The last term on the right-hand side of this equation ($-\gamma X$) represents the rate of endogenous respiration and is explained in more detail in the discussion. The final equation (5d) expresses the microbial growth rate as a function of 2OHQ concentration; because no energy or carbon for growth is obtained from the transformation of quinoline to 2OHQ, it is assumed that the microbial growth rate is not a function of quinoline concentration.

Model Evaluation

Numerical Methods

Solving the set of equations proposed above (equations 3 and 5) involves a numerical treatment of the advective and dispersive fluxes of aqueous species and of the kinetic reactions that change the mass distribution of these aqueous species. Because the rate of reactions with the aqueous components is concentration-dependent, it is important to keep numerical dispersion at a minimum. Large concentration gradients have been observed in subsurface environments, and the sharp interface maintained by these gradients has been implicated as important to controlling reactions [e.g., *Moltz et al.*, 1988; *Smith et al.*, 1991]. Consequently, the numerical techniques employed for solving these problems should have the ability to maintain large concentration gradients if any are present. Other complications that arise in solving the set of equations described above are that (1) the problem is nonlinear as a result of the reactions, and (2) the characteristic time scale at which the reactions occur is much smaller than the characteristic time scale of transport.

The numerical methods used to conduct these simulations were chosen specifically to address these difficulties. The approach de-couples the transport portion of the equations from the reaction portions, by first solving the transport problem given by equations (3) with the source/sink term set to zero. The transport equations are solved by a finite-element modified method of characteristics (MMOC) [*Chiang et al.*, 1989], which has the desirable ability to handle large concentration gradients. The concentrations obtained from this step are then used as the initial concentrations to solve the reaction equations (5), which are treated as ordinary differential equations and are solved with a second-order, explicit Runge-Kutta method with time steps that are generally much smaller than those used for transport. This scheme, in which the reactions are solved separately from the transport problem, is known conventionally as operator splitting and is described in more detail by *Wheeler and Dawson* [1988] and *Valocchi and Malmstead* [1992]. A steady-state velocity field was used to conduct the transport simulations; the velocity field was calculated using a higher-order mixed finite-element method described in detail by *Chiang et al.* [1991].

Although there is no analytical solution for equations (3a-c) coupled with equations (5a-d), the accuracy of the operator-splitting technique was assessed by comparison with the analytical solution for transport with a first-order reaction [*Parker and van Genuchten* 1984] and heuristically by convergence analysis. The code was compared to the analytical solution for convection and dispersion of a single species undergoing a first-order reaction of the form $\Gamma = \mu SX$ for a case with constant X (i.e., no microbial growth). The results of this comparison and the parameters used to generate these results are shown in Figure 3. The time-step sizes used for the flow cell simulations were determined by convergence analysis; the length of the time steps for

transport and for reactions were decreased in a sequence of simulations until the difference between simulations was below a specified tolerance; these time-step values were then used for flow cell simulations.

Simulation of Flow Cell System

The validity of the microbial kinetic model presented above was tested by comparing the simulation results to the laboratory results from the flow cell system. For these simulations, the boundary condition at the inlet was a specified concentration, and the boundary at the outlet was a zero concentration gradient; concentration values for the inflow boundary and the initial conditions appear in Table 1. Values of the physical parameters used in the simulations appear in Table 2, and kinetic parameters for equations (5a-d) used to conduct these simulations appear in Table 3. The results of model simulations appear as breakthrough curves in Figure 4. These breakthrough curves show the concentrations of quinoline, 2OHQ, and oxygen at various longitudinal locations as a function of time for points in the high-K layer (z=19cm), interface (z=16 cm), and low-K layer (z=10 cm).

The porous media in the flow cell were packed carefully to minimize the influence of hydraulic (other than layering) and microbiologic heterogeneities. However, some heterogeneities were undoubtedly present in the system because of the difficulty in packing large volumes of porous media homogeneously. The scatter in the data presented in Figure 4 is due in part to uncertainly in the analyses of the aqueous-phase constituents; however, hydraulic heterogeneity within layers and heterogeneities associated with the initial distribution of microorganisms may also contribute to this scatter.

For the simulations shown, it was assumed that the initial concentration

of microorganisms in the flow cell was uniform throughout both the low-*K* and high-*K* layers. Because the experiment described herein was concerned with processes occurring near the hydraulic layer interface, initially there were no microorganisms in the high-*K* layer. However, it is apparent from examination of the breakthrough curves that there was an appreciable number of organisms in this layer when the biodegradation experiment began. These organisms were probably transported to this layer by the processes of advection and dispersion during tracer experiments conducted before the biodegradation experiment began. Although previous experiments [*Truex et al.*, 1992] and monitoring of the flow cell effluent showed that, at velocities similar to those present in the biodegradation exeriment, the microorganism 866A remains strongly attached to the porous medium, during the tracer experiments, velocities in both layers were approximately 45 times greater than during the biodegradation experiments. At these higher velocities, organisms near the hydraulic layer interface may have been mobilized, although velocities deep in the low-*K* layer remained low enough that mobilization would not have occurred there. The consequence was that the actual distribution of organisms in the high-*K* layer was not accurately known at the start of the biodegradation experiment. Regardless of the difficulties associated with the uncertainty of the initial concentration of microorganisms in the high-*K* layer, the data from the high-*K* layer provide useful information about the processes occurring there; however, simulations of these data must be interpreted with some caution.

In the high-*K* layer, the flow cell data for quinoline show rapid breakthrough (relative to the low-*K* layer) followed by transformation to 2OHQ; the concentration of quinoline eventually levels off because oxygen limitations prevent further transformation, as indicated by the lack of

oxygen in the sytem at these locations (Figure 4a, b). Although the initial concentration of microorganisms was estimated to be equal to the concentration in the low-K layer, the simulations for this region matched the trends of the data well. There was, however, some discrepancy between simulated and observed concentrations for simulations at x=20 cm (Figure 4a). At this location, the simulated rate of quinoline transformation does not appear to be large enough to match the observed data; this results in the simulated production rate of 2OHQ and rate of oxygen utilization also being too low. Simulations for the x=70 cm position matched the observed data better than those for the x=20 cm location.

Near the interface (z=16 cm, 1 cm below the bottom of the high-K layer), simulations generally match the observed data better than for the high-K layer (Figures 4c, d, e). The importance of transverse dispersion is particularly evident near this interface, where the flux of aqueous components from transverse dispersion greatly affects the shape of the breakthrough curves. Simulations matched the observed 2OHQ breakthrough curves near the interface region; however, simulations of the quinoline data indicate a concentration pulse between approximately 0 and 100 hours that did not appear in the observed data. This concentration pulse appears to be a result of the overestimation of quinoline concentrations in the high-K layer, resulting in an overestimation of the transverse dispersive flux into the low-K layer.

Simulations of the low-K layer reflected several trends in the observed data. The effects of the endogenous oxygen uptake term in equation (5c) can be seen clearly in these breakthrough curves (Figure 4f, g, h). The organisms used for this experiment were initially grown on nutrient-rich media, which may have allowed the organisms to store some carbon. When external

carbon sources are lacking, such endogenous carbon can be degraded as an energy source to maintain cellular processes; it is this endogenous respiration that causes the oxygen concentration to drop at a constant rate before any quinoline or 2OHQ is present. For the range of oxygen concentrations simulated, a first-order model for endogenous oxygen uptake represented the observed data well.

The effects of microbial lag are illustrated by the data in Figure 4f, g, h. The pulse of quinoline that travels through the low-K layer is a result of the effect that the lag phase has on the reactions given by equations (5a-d). Because once quinoline has been introduced some time is required for the organisms in any volume of porous medium to induce the quinoline-degrading pathways, some of the quinoline is transported through the volume before degradation begins. Then, once degradation starts, quinoline is metabolized to produce 2OHQ. The result is that some of the quinoline initially injected as a front escapes complete degradation and moves through the system as a high-concentration pulse. The effect of explicitly modeling the lag phase can be seen by comparing the results of simulations that accounted for lag to results of those that did not. Figure 5 shows the results of such a comparison for the low-K layer at x=20 cm. The inclusion of microbial lag accounts for the transient pulse that moves through the system. Although all other microbial parameters are the same for the two simulations, the simulation in which lag was accounted for also maintains a higher concentration at long times.

For both the observed and simulated breakthrough curves, dispersion causes continual spreading of the leading edge of the pulse. This spreading allows a slightly longer contact time with any fixed point in the porous medium (as the residence time of this spreading pulse increases), resulting

in continual degradation of the mass at the trailing end of the pulse (e.g., Figure 4f, g, h). This process keeps the trailing edge of the quinoline pulse sharp, and the effects of dispersion are not as apparent as for the case with no reactions. These results illustrate one case in which it is important to keep numerical dispersion at a minimum to properly represent the kinetic process.

Measured and simulated microbial concentrations at 300 hours are compared as vertical cross-sections in Figure 6 (x=20, 40, and 70 cm). An increase in microbial concentration in the low-K layer near the hydraulic layer interface was observed (Figure 6); it is hypothesized that this increase is a result of transverse dispersive mass fluxes of quinoline, 2OHQ, and oxygen from the high-K layer. The simulated microbial concentrations also showed this trend, although the simulations show more growth in the high-K layer than did the observations. The difference between the observed and simulated microbial concentrations for the high-K layer is probably a result of the uncertainty in the initial microbial concentration there. A total of 53 samples were collected for measurement of microbial concentration at various locations within the flow cell. The observed final distribution of organisms and the final distribution of organisms from the simulations were correlated, although not strongly (r=0.7).

Summary and Conclusions

Microbial kinetic models used for flow cell simulations were developed by observations of the microbial system in independent experiments. The specific growth rate (μ) determined from experiments conducted in batch (free-floating organisms) was different from that determined from

experiments conducted in columns with porous media (attached organisms). Therefore, the specific growth rate was determined from experiments done in porous media. These kinetics were incorporated into a single-phase model, which yielded reasonably accurate simulations of the observed data. For conditions where the microbial concentration is low, a single-phase model may be appropriate, as illustrated in the Appendix.

One of the processes that was identified as being important to describing the microbial kinetics of the experimental system was metabolic lag. A means of describing lag was included in the mathematical model of the microbial kinetics. Comparisons of flow cell simulations conducted with and without the inclusion of metabolic lag in the kinetic description showed that it was important to account for this process to properly describe some aspects of the observed concentrations. In particular, the inclusion of microbial lag allowed the simulation of transient pulses of quinoline that were observed to move through the low-*K* layer.

Observations of microbial concentration in the low-*K* layer showed increases near the hydraulic layer interface. Increased growth near the hydraulic layer interface is hypothesized to result from transverse mass transfer of substrate from the high-*K* layer; because both substrate (as a result of transverse dispersion) and oxygen (which was present initially) are present at this interface, growth can occur in this region, even before the arrival of substrates from advection in the low-*K* layer. The flow cell simulations showed an increase in microbial concentration in the low-*K* layer near the hydraulic layer interface; however, the simulations also showed a correspondingly high concentration in the high-*K* layer that was not observed in the lab data. The small correlation between simulations and observation of microbial concentration in the high-*K* layer was probably a

result of uncertainties in both the initial microbe concentration in this layer and the techniques used to quantify microbial concentration.

Appendix: Comparison of Single-Phase and Two-Phase Models for Microbial Kinetics in Porous Media

For the most general case, transport models that include biodegradation must also include the effects of mass-transport limitations between an immobile microbial phase and the bulk aqueous phase (i.e., formulated as a two-phase model). Below we will show that, for cases in which the microbial concentration is small enough, a single-phase model may be warranted. Development of these arguments begin with the formulation of a two-phase model. The following assumptions are made about the microbial phase in the formulation of the model: (1) biofilms are fully penetrated (i.e., the concentrations of aqueous species within the immobile region are uniformly distributed), (2) the area covered by the microbial phase is directly proportional to the microbial mass [e.g., *Widdowson et al.*, 1988; *Baveye and Valocchi*, 1991], and (3) the transport between the mobile and immobile phases can be represented by a linear diffusion model for which a macroscopic mass-transfer coefficient can be established. The macroscopic mass-transfer coefficient is empirical; it represents the combined effects of the diffusive resistance and geometry of the problem and does not necessarily have a strict physical interpretation.

Given these assumptions, and using a simple one-substrate Monod model for the microbial kinetics, the mass-balance equations for the mobile and immobile phases are given by the following set of equations:

$$\frac{\partial(\theta_m C_m)}{\partial t} = \nabla \cdot (\theta_m \mathbf{D_m} \nabla C_m - \theta_m C_m \mathbf{V_m}) - \eta X \kappa (C_m - C_{im}) \tag{A1}$$

$$\frac{\partial(\theta_{im} C_{im})}{\partial t} = \eta X \kappa (C_m - C_{im}) - \frac{\mu X}{Y} \frac{C_{im}}{C_{im} + K_s} \tag{A2}$$

$$\frac{\partial X}{\partial t} = \mu X \frac{C_{im}}{C_{im} + K_s} \tag{A3}$$

where θ_m and θ_{im} are the volumetric fractions of the mobile and immobile phases, respectively; C_m and C_{im} are the substrate concentrations in the mobile and immobile phases, respectively; η [L^2 M^{-1}] is a parameter that relates microbial concentration to microbial surface area; κ [L T^{-1}] is a coefficient for mass transfer between the mobile and immobile phases; and all other variables and parameters are as described in the body of this paper.

A two-phase model, such as that given by equations (A1) to (A3) should reduce to an analogous single-phase model when values of the mass-transfer rate coefficients are large enough. Equations (A1) to (A3) appear in dimensionless form below; for simplicity, the analysis is formulated in terms of the 1-dimensional problem:

$$\frac{\partial(\theta_m C_m')}{\partial \tau} = \frac{1}{DaI}\left[\frac{1}{Pe}\frac{\partial}{\partial Z}\left(\frac{\partial C_m'}{\partial Z}\right) - \frac{\partial C_m'}{\partial Z}\right] - \frac{X'}{DaII}(C_m' - C_{im}') \tag{A4}$$

$$\frac{\partial(\theta_{im} C_{im}')}{\partial \tau} = X'\left[\frac{1}{DaII}(C_m' - C_{im}') - \frac{C_{im}'}{C_{im}' + K_s'}\right] \tag{A5}$$

$$\frac{\partial X'}{\partial \tau} = \omega X' \frac{C_{im}'}{C_{im}' + K_s'} \tag{A6}$$

where

$$C_m' = \frac{C_m}{C_o} \qquad C_{im}' = \frac{C_{im}}{C_o}$$

$$K_s' = \frac{K_s}{C_o} \qquad Pe = \frac{V_m L}{D_m}$$

$$DaI = \frac{\mu L}{\omega V_m} \qquad DaII = \frac{\mu}{\omega X_o \eta \kappa}$$

$$\tau = \frac{\mu t}{\omega} \qquad X' = \frac{X}{X_o}$$

$$Z = \frac{z}{L} \qquad \omega = \frac{C_o Y}{X_o}$$

$$\theta_{im} = \beta X$$

In the expressions above, C_0 is a reference concentration [M L^{-3}] (the concentration of the substrate at the inlet boundary for the simulations shown below), z [L] is the space variable, and L [L] is a characteristic length for advective transport (conventionally taken to be the distance between the source and observation points). It was assumed that the volume of the mobile region could be taken to be constant (i.e., $\theta_m >> \theta_{im}$), and that the volume of the immobile region could be expressed as being proportional to the microbial concentration (i.e., $\theta_{im} = \beta X$).

Examination of the model given by equations (A4) to (A6) shows the relative importance of transport in the mobile phase, transport between phases, and reactions. For this system of equations to approach an equivalent single-phase system, the following must be true: (1) the characteristic time for transport between phases must be much smaller than the characteristic time for transport, and (2) the characteristic time for transport between phases must be smaller than the characteristic time for the reactions. These two requirements mean essentially that the local equilibrium assumption [LEA] can be applied with respect to the inter-phase transport process [cf. *Valocchi*, 1985; *Bahr and Rubin*, 1987]. The comparison of these "characteristic" times for 1-dimensional systems has conventionally

been done by defining two unitless groupings, known as Damkohler I and Damkohler II numbers [e.g., *Rosner*, 1986; *Baily and Ollis*, 1986]; these groupings are defined above as *DaI* and *DaII*, respectively. The Damkohler I number compares the characteristic time for advective (mobile-phase) transport to that for interphase (mobile to immobile phase) transport, and the Damkohler II number compares the characteristic time for interphase transport to that for reactions within the immobile phase.

To identify cases for which mass-transfer limitations need to be considered, equations (A4) to (A6) were solved in a 1-dimensional simulation for a range of values for *DaII*, and a constant value for *DaI*. In these simulations, the value of *DaI* was near 0.2, so that the LEA cannot be applied with respect to the coupling of advective transport and reactions (i.e., the kinetics of the system must be represented explicitly; cf. *Valocchi*, 1985). The following initial conditions were used for the simulations: $C'_m(0,\tau) = 1$, $C'_{im}(x,0) = 0$, and $X'(x,0) = 0.3$. Boundary conditions for these simulations were the same as those described for the flowcell simulations, and the following parameter values were used: $DaI = 0.2$, $Pe = 170$, $K'_S = 0.005$, $\omega = 50$, $L = 20$ cm, $\beta = 0.01$ cm^3 mg^{-1}. The value picked for X' corresponds to a microbial population density of approximately 10^6 cells per cubic centimeter of porous medium.

Results of these simulations of the mobile phase appear in Figure A1. As the magnitude of *DaII* decreases, the concentration in the mobile phase approaches that given by a single-phase model with equivalent microbial parameters. This suggests that for small enough values of *DaII*, a single-phase model will give results that are a close approximation to the results that would be obtained from a two-phase model. In the case described here, there was at most a 5% difference between the two-phase model and a single-

phase model for $1/DaII > 14$.

The applicability of a single-phase model for simulation of the flow cell experiments can be determined by making a conservative estimate of *DaII*. A value for κ was estimated by using a relation suggested by *Widdowson et al.* [1988], who give $\kappa = D_s^*/\delta$, where D_s^* is the molecular diffusion coefficient [$L^2\ T^{-1}$], and δ [L] is a measure of the effective thickness of the diffusion-limiting region. The value of δ was taken to be 5 μm. This value is on the order of 5 times the dimension of a typical bacterium and results in a conservatively large estimate of the maximum mass-transfer limitation for the microbial concentrations used in the flow cell system. Using the value of the diffusion coefficient for quinoline given in Table 2, κ was calculated to be 1.0 cm s^{-1}. A value of 110 was calculated for η from the parameters used by *Widdowson et al.* [1988]. A value for *DaII* must be calculated for each of the reaction steps given by equation (4); because the reaction given by equation (4a) is in first-order rather than a Monod form, the expression for *DaII* presented above must be modified. Although the details of deriving *DaII* for the first-order reaction case are not given here, it can be shown that $DaII = (\eta\kappa/k)$ [e.g., *Rosner*, 1986]. Using the information given above and that contained in Tables 1, 2, and 3, the values of $1/DaII$ for the reactions given by equations (4a) and (4b) under the conditions present in the flow cell experiments are calculated to be 110 and 1700, respectively. The magnitude of these values indicates that the characteristic time for mass transfer between the mobile and immobile regions is much smaller than the characteristic time for reactions, and a single-phase model appears to be justified.

Acknowledgments. This research was supported by the Subsurface Science

Program, Office of Health and Environmental Research, U.S. Department of Energy (DOE). The continued support of F. J. Wobber is appreciated. Pacific Northwest Laboratory is operated for DOE by Battelle Memorial Institute under Contract DE-AC06-76RLO 1830. The authors also thank M. Truex for his assistance with experiments and information about the bacterium 866A. A. J. Valocchi and M. Malmstead are thanked for information relating to modeling the reactions of 866A with quinoline. M. F. Wheeler is gratefully acknowledged for providing the flow and transport code. The first author is grateful for the helpful discussions with C. S. Simmons in the development of Appendix material.

REFERENCES

Bahr, J., and J. Rubin, Direct comparison of kinetic and local equilibrium formulations for solute transport affected by surface area reactions, *Water Resour. Res.*, *23*, 438-452, 1987.

Baily, J. E., and Ollis, D. F., *Biochemical Engineering Fundamentals*, Second Edition, 984 pp., McGraw-Hill, New York, 1986.

Balkwill, D. L., J. K. Fredrickson, and J. M. Thomas, Vertical and horizontal variations in the physiological diversity of the aerobic chemoheterotrophic bacterial microflora in deep southeast coastal plain subsurface sediments, *Appl. Environ Microbiol.*, *55*, 1058-1065, 1989.

Baveye, P., and A. Valocchi, An evaluation of mathematical models of the transport of biologically reacting solutes in saturated souls and aquifers, *Water Resour. Res.*, *25*, 1413-1421, 1989.

Baveye, P., and A. Valocchi, Reply to "Comment on an evaluation of

mathematical models of the transport of biologically reacting solutes in saturated soils and aquifers", *Water Resour. Res., 27,* 1379-1380, 1991.

Bear, J., *Dynamics of Fluids in Porous Media,* 764 pp., Dover, New York, 1972.

Bird, R. B., W. E. Stewart, and E. N. Lightfoot, *Transport Phenomena,* 780 pp., Wiley, New York, 1960.

Borden, R. C., and P. B. Bedient, Transport of dissolved hydrocarbons influenced by oxygen-limited biodegradation, 1. Theoretical development, *Water Resour. Res., 22,* 1973-1982, 1986.

Bouwer, E. J., and P. McCarty, Modeling of trace organics biotransformation in the subsurface, *Ground Water, 22,* 433-440, 1984.

Brockman, F. J., B. A. Denovan, R. J. Hicks, and J. K. Fredrickson, Isolation and characterization of quinoline-degrading bacteria from subsurface sediments, *App. and Env. Microbiol. 55,* 1029-1032, 1989.

Chiang, C. Y., M. F. Wheeler, and P. B. Bedient, A modified method of characteristics technique and a mixed finite element method for simulation of groundwater solute transport, *Water Resour. Res., 25,* 1541-1549, 1989.

Chiang, C. Y., C. N. Dawson, and M. F. Wheeler, Modeling of in-situ biorestoration of organic compounds in groundwater, *Transport in Porous Media, 6,* 667-702, 1991.

Coats, K. H., and B.D. Smith, Dead-end pore volume and dispersion in porous media, *Soc. Petrol. Eng., J., 4,* 73-84, 1964.

Colwell, F. S., Microbiological comparison of surface soil and unsaturated subsurface soil from a semiarid high desert, *Appl. Environ. Microbiol., 55,* 2420-2423, 1989.

Contois, D. E., Kinetics of bacterial growth: Relationships between

population density and specific growth rate in continuous culture, *J. Gen. Microbiol., 21*, 40-50, 1959.

Dabes, J. N., R. F. Finn, and C. R. Wilke, Equations of substrate-limited growth: the case for blackman kinetics, *Biotechnol. Bioeng., 15*, 1159-1177, 1973.

De Smedt, F., and P. J. Wierenga, Mass transfer in porous media with immobile water, *J. Hydrol., 41*, 59-67, 1979.

Edwards, V. H., The influence of high substrate concentrations on microbial kinetics, *Biotechnol. Bioeng., 12*, 679-712, 1970.

Fredrickson, J. K., D. L. Balkwill, J. M. Zachara, S.-M. W. Li, F. J . Brockman, and M. A. Simmons, Physiological diversity and distributions of heterotrophic bacteria in deep Cretaceous sediments of the Atlantic coastal plain, *Appl. Environ. Microbiol.*, 57, 402-411, 1991.

Gaudy, A. F., and E. T. Gaudy, *Elements of Bioenvironmental Engineering*, 592 pp., Engineering Press, Inc., San Jose, California, 1988.

Harvey, R. W., R. L. Smith, and L. George, Effect of organic contamination upon microbial distributions and heterotrophic uptake in a Cape Cod, Mass., aquifer, *Appl., Environ. Microbiol., 48*, 1197-1202, 1984.

Hirsch, P., and E. Rades-Rohkohl, Some special problems in the determination of viable counts of groundwater microorganisms, *Microb. Ecol., 16*, 99-113, 1988.

Kindred, J. S., and M. A. Celia, Contaminant transport and biodegradation, 2. conceptual model and test simulations, *Water Resour. Res., 25*, 1149-1159, 1989.

Kinzelbach, W., W. Schafer, and J. Herzer, Numerical modeling of nitrate and enhanced denitrification processes in aquifers, *Water Resour. Res., 27*, 1123-1135, 1991.

Kono, T., Kinetics of microbial cell growth, *Biotech. Bioeng., 10,* 105-131, 1968.

Lee, J.M., *Biochemical Engineering,* 321 pp., Prentice-Hall, Englewood Cliffs, New Jersey, 1992.

Malmstead, M. J., Modeling oxygen-dependent biodegradation of quinoline in batch and column systems, M. S. thesis, 131 pp., University of Illinois, Urbana-Champaign, Illinois, 1992.

Madsen, E. L., Determining in situ biodegradation, *Environ. Sci. Technol., 25,* 1663-1673, 1991.

Madsen, E. L., and W. C. Ghiorse, Ground water microbiology: subsurface ecosystem processes, in *Aquatic Microbiology: An Ecological Approach,* T. Ford, ed, Blackwell Scientific Pub. Inc., Cambridge, Massachusetts, 1992.

McBride, J. F., F. J. Brockman, J. E. Szecsody, and G. P. Streile, Kinetics of quinoline degradation, sorption, and desorption in a clay-coated model soil containing a quinoline degrading bacterium, *J. Contam. Hydrol., 9,* 133-154, 1992.

MeGee, R. D., S. Kinoshita, A. G. Fredrikson, and H. M. Tsuchiya, Differentiation and product formation in molds, *Biotechnol., Bioeng., 12,* 771-801, 1970.

Moltz, F. J., and M. A. Widdowson, Internal inconsistencies in dispersion-dominated models that incorporate chemical and microbial kinetics, *Water Resour. Res., 24,* 615-619, 1988.

Moltz, F. J., M. A. Widdowson, and L. D. Benefield, Simulation of microbial growth dynamics coupled to nutrient and oxygen transport in porous media, *Water Resour. Res., 22,* 1207-1216, 1986.

Monod, J., The growth of bacterial cultures, *Ann. Rev. Microbiol., 3,* 371-393, 1949.

Moser, H., The dynamics of bacterial population maintained in the chemostat, *Carnegie Inst. Wash. Pub. No. 614*, 1958.

Olson, B. H., R. McCleary, and J. Meeker, Background and models for bacterial biofilm formation and function in water distribution systems, in *Modeling the Environmental Fate of Microorganisms*, pp. 255-285, American Society for Microbiology, Washington, D.C., 1991.

Pamment, N. B., Absence of external causes of lag in *Saccharomyces cerevisiae*, *J. Gen. Microbiol., 105*, 297-304, 1978.

Parker, J. C. and M. Th. van Genuchten, Determining transport parameters from laboratory and field tracer experiments, *Bulletin 84-3*, 97 pp., Virginia Agricultural Experiment Station, Blacksburg, Virginia, 1984.

Pereira, W. E., C. Rostad, J. Garbarino, and M. Hult, Groundwater contamination by organic bases derived from coal-tar wastes, *Environmental Toxicology and Chemistry, 2*, 283-294, 1983.

Powell, E. O., The growth rate of microorganisms as a function of substrate concentration, in *Microbial Physiology and Continuous Culture*, edited by E. O. Powell, C. G. T. Evans, R. E. Strange, and D. W. Tempest, pp. 34-56, Her Majesty's Stationery Office, London, 1967.

Ramkrishna, D., A. G. Fredrickson, and H. M. Tsuchiya, The dynamics of microbial propagation, models considering inhibitors and valuable cell composition, *Biotechnol. Bioeng., 9*, 129-170, 1967.

Rittman, B. E., P. L. McCarty, and P. V. Roberts, Trace-organics biodegradation in aquifer recharge, *Ground Water, 18*, 236-243, 1980.

Robbins, G. A, Methods for determining transverse dispersion coefficients of porous media in laboratory column experiments, *Water Resour. Res., 25*, 1249-1258, 1989.

Roels, J. A., *Energetics and Kinetics in Biotechnology*, 330pp., Elsevier,

Amsterdam, 1983.

Rosner, D. E., *Transport Processes in Chemically Reacting Flow*, 540 pp., Butterworths, Boston, 1986.

Severson, K. J., D. L. Johnstone, C. K. Keller, and B. D. Wood, Hydrogeologic parameters affecting vadose-zone microbial distributions, *Geomicrobiol. J., 9*, 197-216, 1992.

Smith, R. L., Harvey, R. W., and D. R. LeBlanc, Importance of closely spaced vertical sampling in delineating chemical and microbiological gradients in groundwater studies, *J. Contaminant Hydrol. 7*, 285-300, 1991.

Stuermer, D. H., D. J. Ng, and C. J. Morris, Organic contaminants in groundwater near an underground coal gasification site in northeastern Wyoming, *Environ. Sci. Technol., 16*, 582, 1987.

Sykes, J. F., S. Soyupak, and G. J. Farquhar, Modeling of leachate organic migration and attenuation in groundwaters below sanitary landfills, *Water Resour. Res., 18*, 135-145, 1982.

Truex, M. J., F. J. Brockman, D. L. Johnstone, and J. K. Fredrickson, Effect of starvation on induction of quinoline degradation for a subsurface bacterium in a continuous-flow column, *Appl. Environ. Microbiol., 58*, 2386-2392, 1992.

Valocchi, A., Validity of the local equilibrium assumption for modeling sorbing phase solute transport through homogenous soils, *Water Resour. Res., 21*, 808-820, 1985.

Valocchi, A., and M. Malmstead, Accuracy of operator splitting for advection-dispersion-reaction problems, *Water Resour. Res., 28*, 1471-1476, 1992.

van Genuchten, M. Th., and P. J. Wierenga, Mass transfer studies in sorbing

porous media, I, Analytical Solutions, *Soil Sci. Soc. Am. J., 40,* 473-480, 1976.

Wheeler, M. F., and C. N. Dawson, An operator-splitting method for advection-diffusion-reaction problems, *MAFELAP Proceedings VI,* 463-482, 1988.

Widdowson, M. A., F. J. Moltz, and L. D. Benefield, A numerical transport model for oxygen- and nitrate-based respiration linked to substrate and nutrient availability in porous media, *Water Resour. Res., 24,* 1553-1565, 1988.

Williams, F. M., A model of cell growth dynamics, *J. Theoret. Biol., 15,* 190-207, 1967.

Wood, B. D., and C. N. Dawson, Effects of lag and maximum growth in contaminant transport and biodegradation modeling, in *Proceedings of the IX International Conference on Computational Methods in Water Resource Modeling,* 2, 317-324, 1992.

FIGURE CAPTIONS

Figure 1. Schematic diagram of the flow cell apparatus. The ratio of the conductivities in the high- and low-*K* layers is approximately 1:13. Sampling ports (represented by dots on the figure) on the side of the flow cell were equipped with needles inserted to the center of the flow cell. Small sample volumes were removed through these ports during the course of the experiment, for analysis of aqueous-phase component concentrations.

Figure 2. Catabolic degradation sequence from quinoline to end products. Because carbon, oxygen, nitrogen, and hydrogen are also taken up during metabolism as a result of anabolic processes, the stoichiometry shown here does not represent the result of the entire reaction.

Figure 3. Comparison of analytical solution of *van Genuchten and Wierenga* [1976] (points) to model results (solid line). This comparison is for three different first-order reaction rate coefficients (μ) with no microbial growth. Parameters used for these simulations are provided on the plot; the units of μ are mg L^{-1} s^{-1}).

Figure 4. Breakthrough curves comparing model results to laboratory data Plots show normalized concentration of quinoline, 2OHQ, and oxygen as a function of time at the specified spatial location.

Figure 5. Plot of quinoline break-through curve in low-*K* layer at x=20 cm

for simulations that include the effects of lag (solid line) and others that do not include the effects of lag (dashed line). The inclusion of lag in the microbial kinetic model allows the simulation of the transient pulse of quinoline that propagates through the system in the low-*K* layer.

Figure 6. Comparison of observed (solid line) and simulated (thick dashed line) vertical distibutions of microbes at 300 hours for three horizontal locations. Concentrations are normalized to the initial microbial concentration as packed in the flow cell. The dashed horizontal line at z=17 cm represents the location of the layer interface.

Figure A1. Breakthrough curves for a two-phase model with varying values of the mass-transfer coefficient (*DaII*). As the mass-transfer coefficient becomes large, the results of the two-phase model approach that of a single-phase model. Where diffusive mass transfer is not expected to be limiting, a single–phase model may adequately describe the system.

Table 1. Concentrations for Boundary and Initial Conditions

Parameter	Value
Inflow Boundary Concentrations	
S_1 [mg L^{-1}]	20
S_2 [mg L^{-1}]	0
O [mg L^{-1}]	9
X [CFU g^{-1}]	0
Initial Condition Concentrations	
S_1 [mg L^{-1}]	0
S_2 [mg L^{-1}]	0
O [mg L^{-1}]	9
X [CFU g^{-1}]	5×10^6

Table 2 . Physical Parameters Used to Model Flow Cell

Parameter	Value	Source*
θ_w	0.4	M
$\alpha_{l,high}$ [m]	8.3×10^{-2}	M
$\alpha_{t,high}$ [m]	2.4×10^{-5}	M
$\alpha_{l,low}$ [m]	1.2×10^{-3}	M
$\alpha_{t,low}$ [m]	4.5×10^{-4}	M
k_{high} [m s^{-1}]	1.6×10^{-3}	M
k_{low} [m s^{-1}]	1.2×10^{-4}	C**
D^* [m^2 s^{-1}]	2.0×10^{-10}	L

* M, measured value; C calculated value; L from *Bird et al.* [1960]

** Conductivity in the low-*K* layer (k_{low}) calculated from measured conductivity in high-*K* layer (k_{high}) and the ratio of the velocities measured by tracer tests

Table 3. Microbial Kinetic Parameters Used to Model Flowcell

Parameter	Value	Source*
k [mg^{-1} L d^{-1}]	1.70	E
K_{o1} [mg L^{-1}]	0.02	L
μ_2 [d^{-1}]	1.70	E
Y_2	0.35	E
K_{s2} [mg L^{-1}]	0.05	L
K_{o2} [mg L^{-1}]	2.00	L
r	1.12	C
f_1	0.15	L
f_2	1.50	E
γ[d^{-1}]	1.0	E
τ_L [d]	0.4	E, L2
τ_E [d]	3.0	E, L2
b [d^{-1}]	0.0	L2

*E, experimental measurement; C calculated value; L1 from *Malmstead* [1992]; L2 from *Truex et al.* [1992]

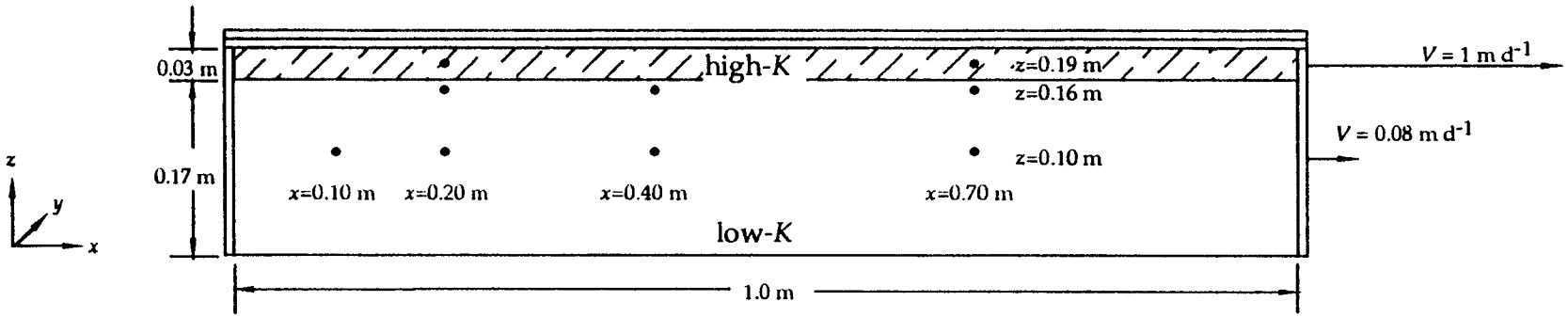
0.03 m
0.17 m
high-K
low-K
z=0.19 m
z=0.16 m
z=0.10 m
x=0.10 m
x=0.20 m
x=0.40 m
x=0.70 m
1.0 m
V = 1 m d-1
V = 0.08 m d-1
z
y
x

FIG 1

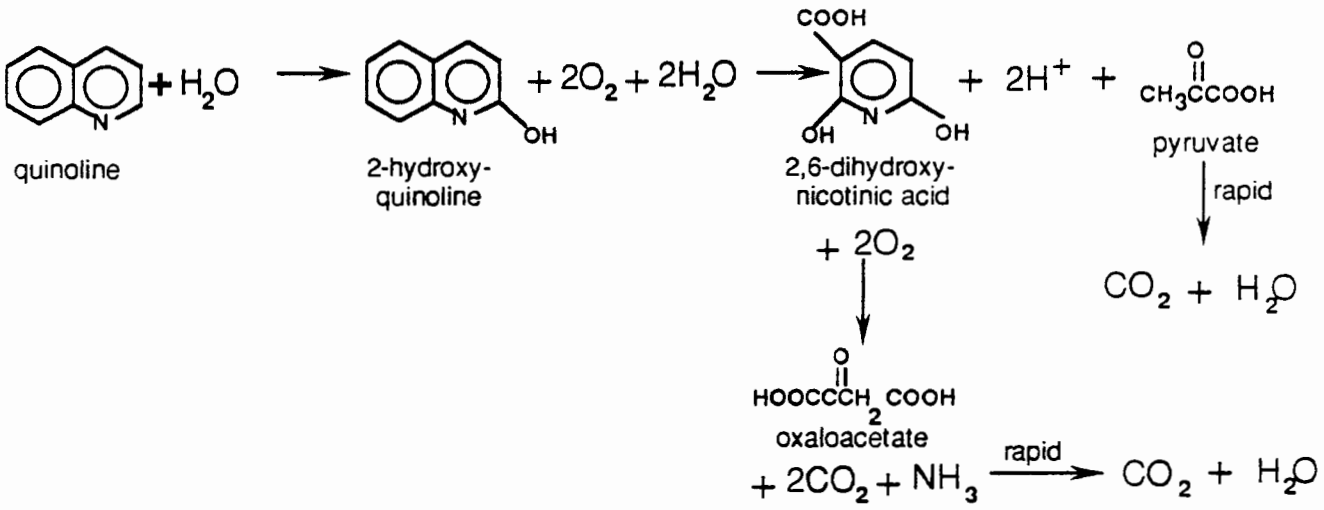
+ H_2O
quinoline
+ $2O_2$ + $2H_2O$
2-hydroxy-quinoline
COOH
OH
N
OH
2,6-dihydroxy-nicotinic acid
+ $2H^+$ +
CH_3CCOOH
pyruvate
rapid
CO_2 + H_2O
+ $2O_2$
$HOOCCCH_2COOH$
oxaloacetate
+ $2CO_2$ + NH_3
rapid
CO_2 + H_2O

FIG 2

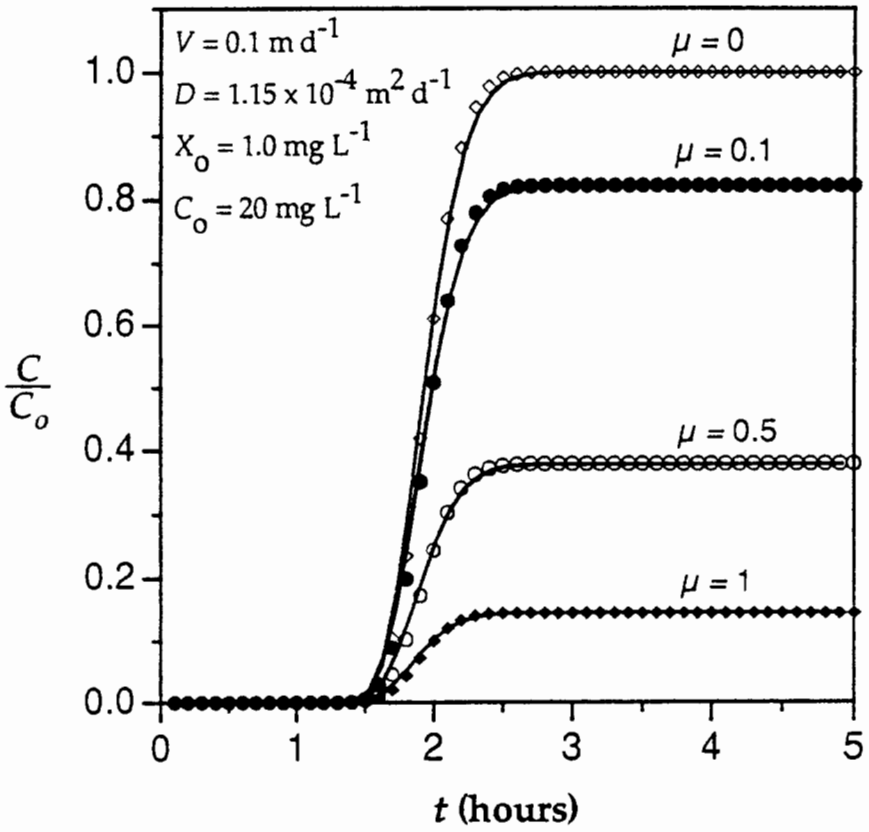
V = 0.1 m d-1
D = 1.15 x 10-4 m2 d-1
Xo = 1.0 mg L-1
Co = 20 mg L-1
μ = 0
μ = 0.1
μ = 0.5
μ = 1
C/Co
t (hours)
0.0
0.2
0.4
0.6
0.8
1.0
0
1
2
3
4
5

Figure 3

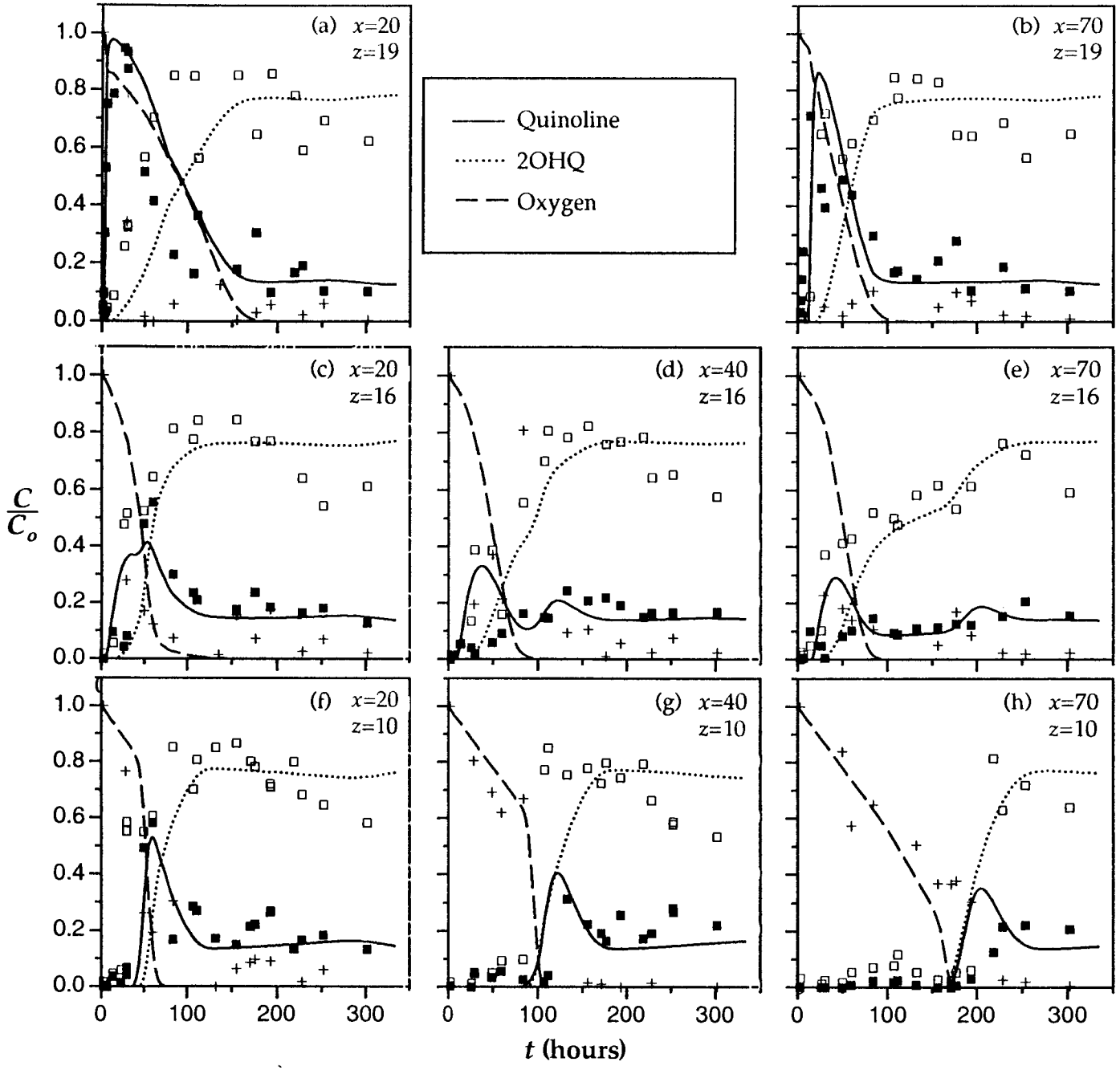
(a) x=20 z=19
(b) x=70 z=19
(c) x=20 z=16
(d) x=40 z=16
(e) x=70 z=16
(f) x=20 z=10
(g) x=40 z=10
(h) x=70 z=10
Quinoline
2OHQ
Oxygen
C/Co
t (hours)
0.0
0.2
0.4
0.6
0.8
1.0
0
100
200
300

Figure 4

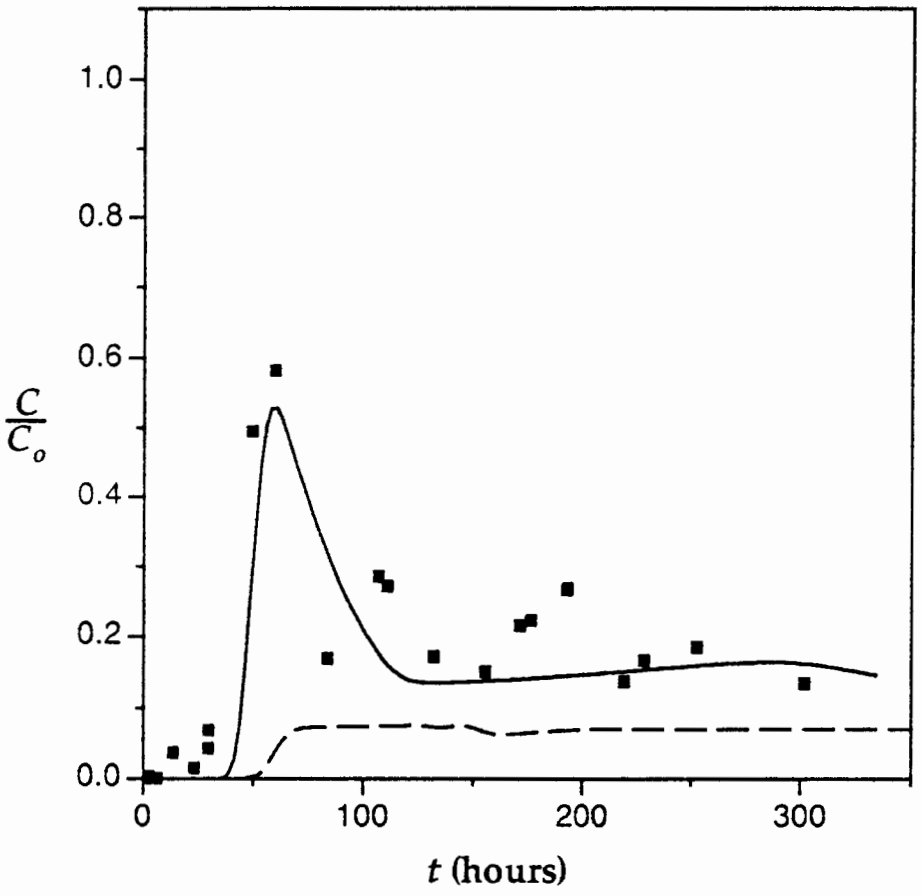

Figure 5

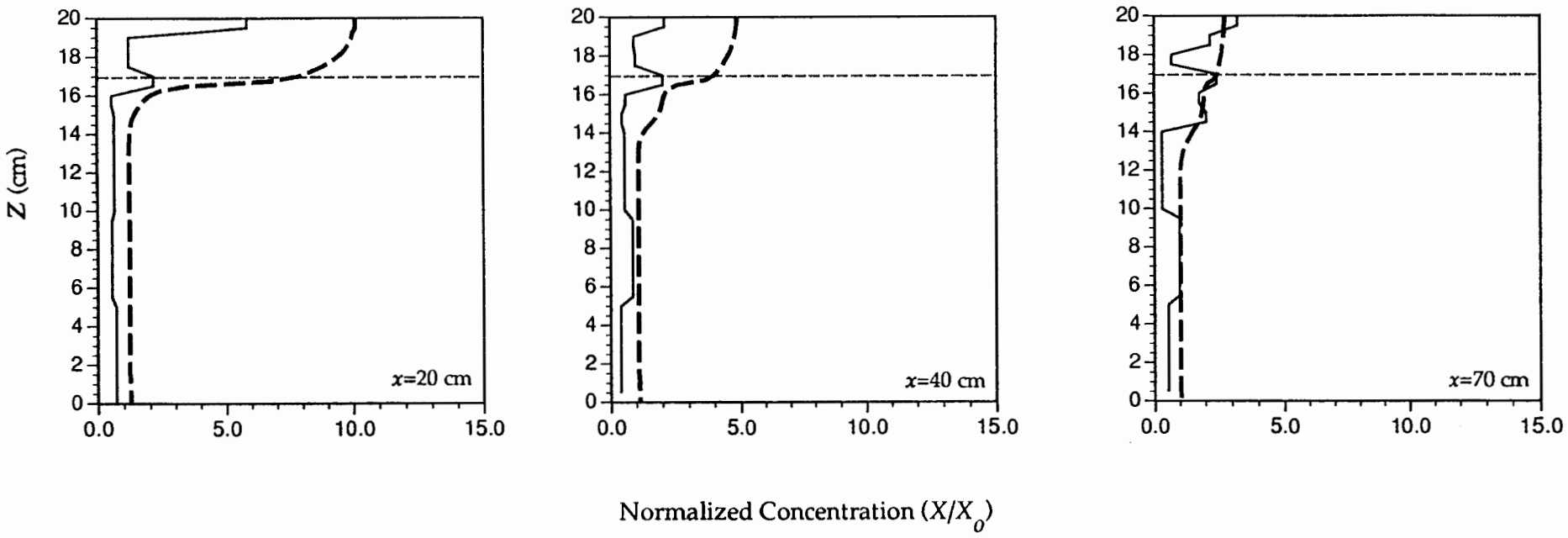

FIG 6

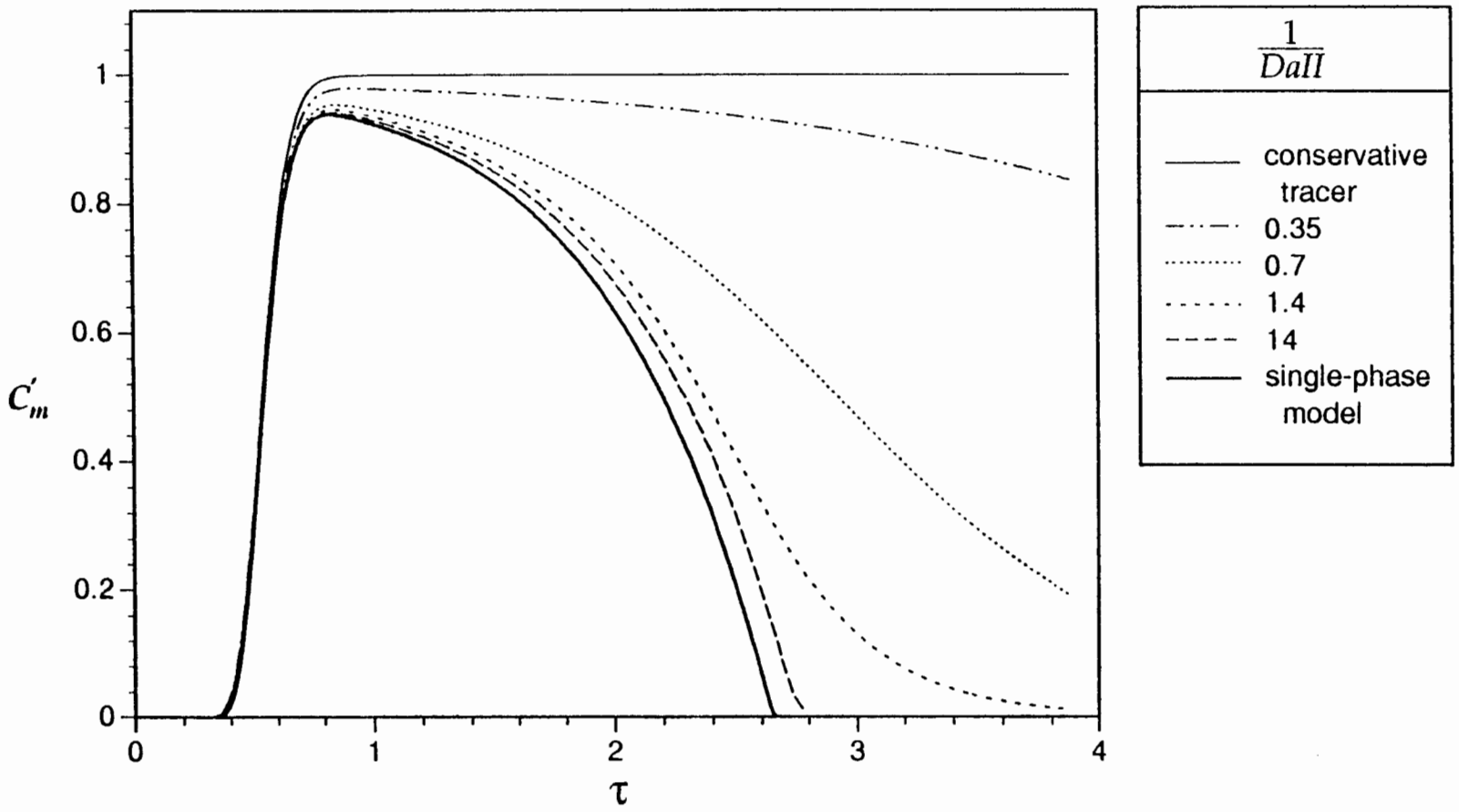
C'_m
1
0.8
0.6
0.4
0.2
0
0
1
2
3
4
τ
$\frac{1}{DaII}$
conservative tracer
0.35
0.7
1.4
14
single-phase model

Figure A1